JBC ARTICLE

Induction of UCP1 and thermogenesis by a small molecule via AKAP1/PKA modulation

Received for publication, March 3, 2020, and in revised form, July 24, 2020 Published, Papers in Press, August 27, 2020, DOI 10.1074/jbc.RA120.013322

Laurent Vergnes[1,*], **Jason Y. Lin**[1], **Graeme R. Davies**[2], **Christopher D. Church**[2], **and Karen Reue**[1,3]

From the [1]*Department of Human Genetics, David Geffen School of Medicine, University of California-Los Angeles, Los Angeles, California, USA, the* [2]*Cardiovascular, Renal and Metabolism, BioPharmaceuticals R&D, AstraZeneca, Cambridge, United Kingdom, and the* [3]*Department of Medicine, and Molecular Biology Institute, University of California-Los Angeles, Los Angeles, CA, USA*

Edited by Lila M. Gierasch

Strategies to increase energy expenditure are an attractive approach to reduce excess fat storage and body weight to improve metabolic health. In mammals, uncoupling protein-1 (UCP1) in brown and beige adipocytes uncouples fatty acid oxidation from ATP generation in mitochondria and promotes energy dissipation as heat. We set out to identify small molecules that enhance UCP1 levels and activity using a high-throughput screen of nearly 12,000 compounds in mouse brown adipocytes. We identified a family of compounds that increase *Ucp1* expression and mitochondrial activity (including uncoupled respiration) in mouse brown adipocytes and human brown and white adipocytes. The mechanism of action may be through compound binding to A kinase anchoring protein (AKAP) 1, modulating its localization to mitochondria and its interaction with protein kinase A (PKA), a known node in the β-adrenergic signaling pathway. In mice, the hit compound increased body temperature, UCP1 protein levels, and thermogenic gene expression. Some of the compound effects on mitochondrial function were UCP1- or AKAP1-independent, suggesting compound effects on multiple nodes of energy regulation. Overall, our results highlight a role for AKAP1 in thermogenesis, uncoupled respiration, and regulation energy balance.

The increasing prevalence of obesity worldwide reflects changes in lifestyle, including a combination of increased food intake and reduced physical activity. Obesity causes complex metabolic, endocrine, and hemodynamic changes that may promote dyslipidemias, cardiovascular disease, and type 2 diabetes (1, 2). Because obesity develops when energy intake exceeds energy expenditure, increasing the latter is an attractive strategy to reduce body weight and fat storage (3, 4).

There has been extensive interest in modulating thermogenesis as a treatment for obesity (5–9). During adaptive thermogenesis, particularly in response to cold exposure, mammals dissipate energy in brown adipose tissue (BAT) as heat by decreasing coupling between fatty acid oxidation and ATP synthesis as well as increasing mitochondrial biogenesis. Stored energy in fat is converted to heat, so changes in mitochondrial respiration or in the level of uncoupling activity could promote fat utilization. Recently, the existence of BAT in humans has been reappraised and there is good evidence that brown fat depots are active in adults and are capable of energy dissipation (10–13). Moreover, adipocytes within white adipose tissue (WAT) may be induced to acquire brown adipocyte characteristics in both animals and humans by recruiting precursor cells or by transdifferentiation (6, 14–17). These beige adipocytes derive from a distinct cellular lineage than brown adipocytes but have a similar multilocular morphology and high respiration rates. Thus, human BAT and browning of WAT may be important regulators of body fat accumulation/utilization and potential anti-obesity drug targets.

One key factor in adaptive thermogenesis in BAT is the mitochondrial uncoupling protein-1 (UCP1). UCP1 is responsible for enabling the protein leak in mitochondria that dissipates energy resulting from oxidative metabolism (18, 19). The presence of UCP1 in both classical brown adipocytes and beige adipocytes has spurred interest in targeting UCP1 as a means of increasing energy expenditure. *Ucp1* expression is induced by stimulation of the sympathetic nervous system during cold exposure through activation of the β-adrenergic receptor. This leads to cAMP production and activation of cAMP-dependent protein kinase (PKA), p38 mitogen-activated protein kinase (p38 MAPK), and transcription factors such as peroxisome proliferator-activated receptor γ (PPARγ), PPARγ coactivator 1α (PGC1α), and activating transcription factor 2 (ATF2) (18, 20–22). PKA activation by the second messenger cAMP is critical for the subsequent post-translational modification of transcription factors that induce a thermogenic gene expression program. The PKA holoenzyme comprises 2 catalytic and 2 regulatory subunits (23). PKA is involved in several signaling pathways and acts in multiple tissues and subcellular compartments. The spatiotemporal organization of PKA activity is facilitated by scaffolding proteins, including protein kinase A anchoring proteins (AKAPs). AKAPs compartmentalize PKA to specific subcellular locations such as the cellular membrane, the nucleus, or the mitochondria, allowing distinct substrate phosphorylation and specific signal transmission (24–26). There has been an interest in targeting AKAPs to influence PKA activity (26, 27).

Although the thermogenic pathway and *Ucp1* transcriptional effectors have been relatively well characterized, few small molecules have been identified that target *Ucp1* expression or

This article contains supporting information.

* For correspondence: Laurent Vergnes, lvergnes@ucla.edu.

Present address for Jason Y. Lin: Department of Genetics and Complex Diseases, HSPH, Boston, Massachusetts, USA.

activation (7, 28–30). In addition, β3-adrenoreceptor agonists such as CL316,243 increase thermogenesis in rats and mice, but they have poor efficacy on the human β3-adrenoreceptor homolog (9, 31). We hypothesized that an unbiased small molecule screen could identify compounds that regulate UCP1 levels or activity by mechanisms other than β3-adrenoreceptor activation. We generated a brown adipocyte cell line containing a reporter for *Ucp1* expression and screened nearly 12,000 small molecules for induction of reporter expression. We identified a family of compounds that effectively induces endogenous UCP1 levels in mouse brown adipocytes and human white adipocytes. A lead compound from this family promotes mitochondria-related gene expression, and activates PKA and lipolysis. Experiments based on protein stabilization suggest that the compound acts by binding AKAP1, thus modifying the PKA signaling pathway in adipocytes.

Results

Identification of small molecules that induce Ucp1 expression

Transcriptional regulation of *Ucp1* has been extensively documented (21, 22). The transcriptional activation of *Ucp1* is driven by two known regulatory regions: a proximal region next to the promoter and an enhancer element located 2.5 kb upstream of the transcription start site. By cross-species sequence comparisons, we noted that additional evolutionarily conserved sequences are present upstream and downstream of the enhancer region (Fig. 1*A*). To assess the functional significance of these conserved elements, we cloned different lengths of the mouse *Ucp1* promoter (2.3, 3, 5, and 7 kb) upstream of a luciferase reporter gene, and established stable brown adipocyte cell lines with each of these constructs. We tested each cell line for luciferase activity in response to known *Ucp1* transcriptional activators: CL316,243 (synthetic β3-adrenergic agonist), forskolin (adenylyl cyclase activator), rosiglitazone (PPARγ agonist), and retinoic acids (retinoic acid receptor agonists). The maximal luciferase activity was observed for the 3-kb *Ucp1* promoter construct, which includes the known enhancer (Fig. 1*B*). Longer sequences had diminished activity, suggesting the presence of negative regulatory elements upstream of the enhancer. Based on these pilot studies, we selected the cell line expressing the 3-kb construct for our small molecule screen. We screened 11,712 compounds (final concentration of 10 μM) in duplicate from a combination of libraries (see "Experimental procedures"). Duplicate samples showed good reproducibility (Fig. S1*A*), providing confidence in the results, even though the Z score achieved with known *Ucp1* inducers such as forskolin were modest (0.193 with forskolin).

Validation of compounds using endogenous Ucp1 expression

For further characterization, we selected compounds showing increased activation over vehicle of >55% for both duplicates (Fig. 1*C*). This group comprised 97 molecules, of which 30% had known functions, including several compounds with adrenergic agonist activity. To validate the compounds, we treated brown adipocytes with 92 compounds (excluding known adrenergic agonists) and measured endogenous *Ucp1* expression by qPCR. Twenty-two compounds induced *Ucp1* expression >2-fold during two independent experiments (Table S1). Most of these compounds also increased expression of *Ppargc1a* and *Pparg*. We selected one compound with unknown function, AST 7062601, for further characterization, with the aims of understanding its mechanism of action.

AST 7062601 (or AST070) is an *N*-(2,3-dihydro-1,4-benzodioxin-6-yl)-2-[(4-oxo-3,4-dihydroquinazolin-2-yl)sulfanyl]acetamide. Titration experiments revealed that AST070 induced *Ucp1* expression optimally at a concentration of 10 μM, with lower induction at 1 μM (Fig. 1*D*). The effect of 10 μM AST070 on *Ucp1* expression was observed as early as 5 h and lasted at least 24 h (Fig. S1*B*). To optimize the lead compound, we selected 25 compounds with more than 81% identity (structures provided in Fig. S2*A*) and assessed their effect on *Ucp1* expression. Many of the 25 compounds induced *Ucp1* expression to a similar level as AST070 and to CL316,243 (Fig. 1*E*). We identified one compound, Z16078526 (Z160), which had greater potency than AST070 on *Ucp1* induction. Both AST070 and Z160 robustly induced endogenous *Ucp1* expression in primary mouse brown adipocytes (29- and 62-fold for AST070 and Z160, respectively; Fig. 2*A*), which was more pronounced than the drug action in immortalized brown adipocytes (Fig. 1*E*). AST070, Z160, and related compounds all contain quinazoline, sulfur, acetamide, and benzene chemical groups. The removal of any of these functional groups blunted the induction of *Ucp1* mRNA (Fig. S2*B*).

AST070 and Z160 promote mitochondrial activation in brown and white adipocytes

We further characterized the effects of AST070 and Z160 on adipocyte metabolism by analyzing gene expression and mitochondrial respiration. Treatment of primary (Fig. 2*A*) and immortalized brown adipocytes (Fig. S3) with AST070 or Z160 promoted expression of markers of brown adipocyte identity (32, 33), and of genes involved in mitochondrial function and fatty acid oxidation. Larger effects were observed in primary compared with immortalized cells. To investigate whether the compounds affected mitochondrial function, we treated brown adipocytes with AST070 and Z160 before assessing mitochondrial respiration with a Seahorse XF analyzer. Both AST070 and Z160 increased mitochondrial respiration, and more specifically, uncoupled respiration (Fig. 2*B*). Maximal respiration was also significantly elevated by AST070, and showed the same trend for Z160, suggesting an increase in mitochondrial reserve capacity. To confirm that the increase in uncoupled respiration was due to UCP1, we isolated mitochondria from cells treated with Z160. The GDP-sensitive respiration, which represent UCP1-dependent respiration, was increased similarly to the total uncoupled respiration, demonstrating the UCP1-dependent leak (Fig. 2*C*).

To validate these findings in a human cellular model, we used an immortalized human brown adipocyte cell line. Z160 induced *UCP1* expression nearly 7-fold, and also increased expression of *CIDEA* (Fig. 3*A*). Importantly, Z160 also increased mitochondrial respiration (primarily uncoupled respiration), as well as maximal respiration, in the human brown adipocyte cell line (Fig. 3*B*). Given that white adipocytes have the ability to express brown adipocyte properties with specific

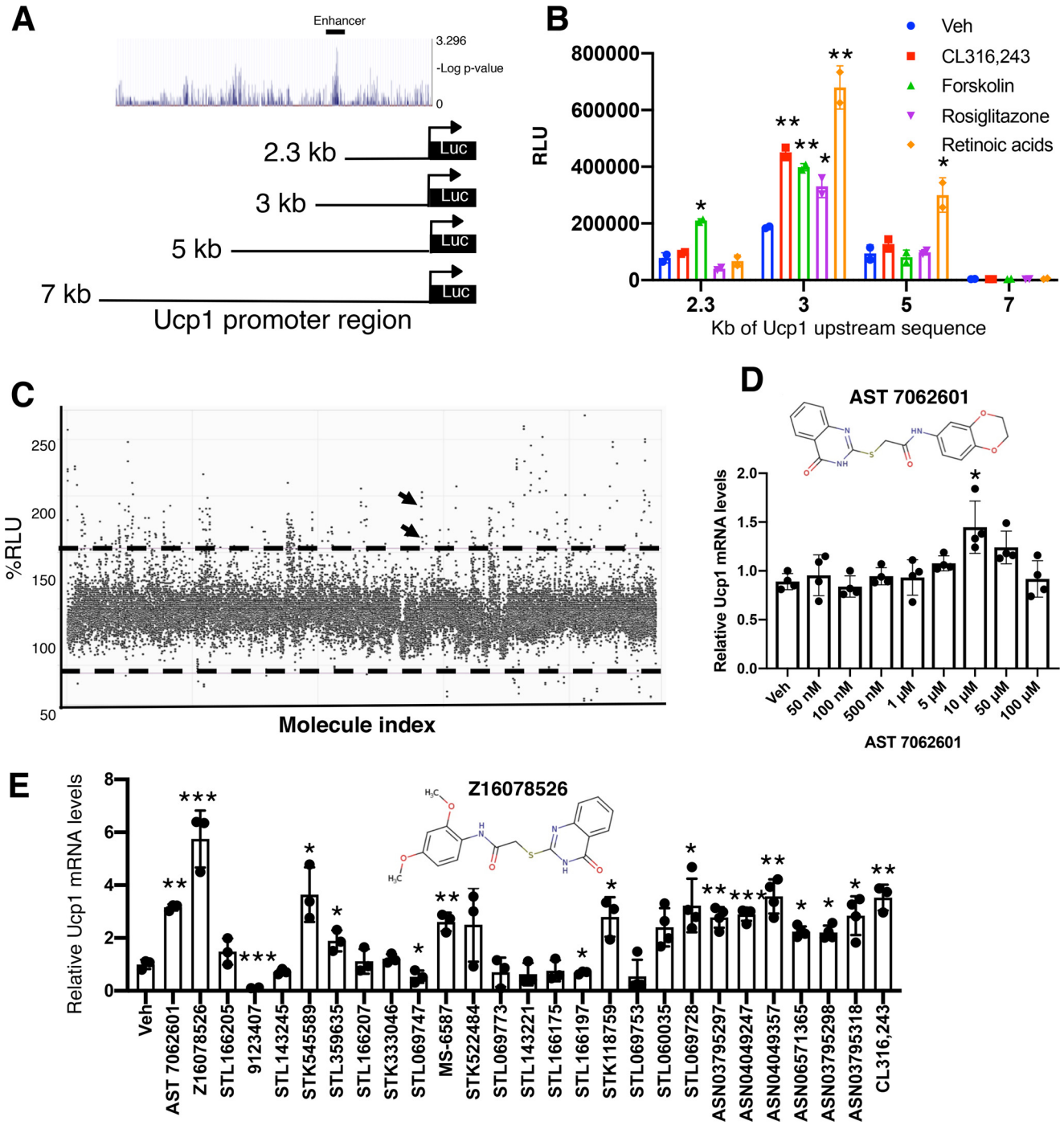

Figure 1. Identification of small molecules that induce *Ucp1* expression in mouse brown adipocytes. *A*, *Ucp1* promoter–luciferase reporter constructs are shown to scale *below* a diagram of evolutionarily conserved regions in the mouse *Ucp1* promoter retrieved from the conservation track in the UCSC genome browser (RRID:SCR_005780). The location of the enhancer is indicated. *B*, luciferase activity (expressed as relative luminometer units, *RLU*) in brown adipocyte cell lines that were stably transfected with *Ucp1* promoter–luciferase constructs shown in *panel A*. Cells were treated overnight with vehicle (*Veh*) or effectors indicated ($n = 2$). *C*, summary of luciferase activity generated in brown adipocyte cell line stably expressing the 3-kb *Ucp1* promoter-luciferase construct from *panel A*. Results are shown for ~12,000 compounds (10 μM), with each *dot* representing the RLU for one compound. *Horizontal dashed lines* represent the arbitrary +/− 55% change from values obtained with vehicle alone. *Arrows* indicate AST 7062601 ($n = 2$). *D*, *Ucp1* mRNA levels from immortalized brown adipocytes after overnight treatment with vehicle or with AST 7062601 at the concentrations indicated ($n = 4$). The AST 7062601 structure is shown *above* the graph. *E*, *Ucp1* mRNA levels after treatment with 10 μM AST 7062601 or other compounds with > 81% identity. Treatment with vehicle and with 10 nM CL316,243 are shown for comparison ($n = 3$-4). The Z16078526 structure is shown *above* graph. All data presented as mean ± S.D. *, $p < 0.05$; **, $p < 0.01$; ***, $p < 0.001$.

metabolic stimuli, we also assessed whether Z160 influences brown adipocyte character in human white adipocytes. Interestingly, Z160 also induced *UCP1* expression 7-fold, and greatly increased expression of *CIDEA*, *ACADM*, *CPT1B*, and *ELOVL3* (Fig. 3*C*). Similarly to the human brown adipocytes, Z160 also increased mitochondrial respiration (uncoupled), as well as maximal respiration, in the human white adipocyte cell line (Fig. 3*D*). Together, these results indicate that Z160 activates

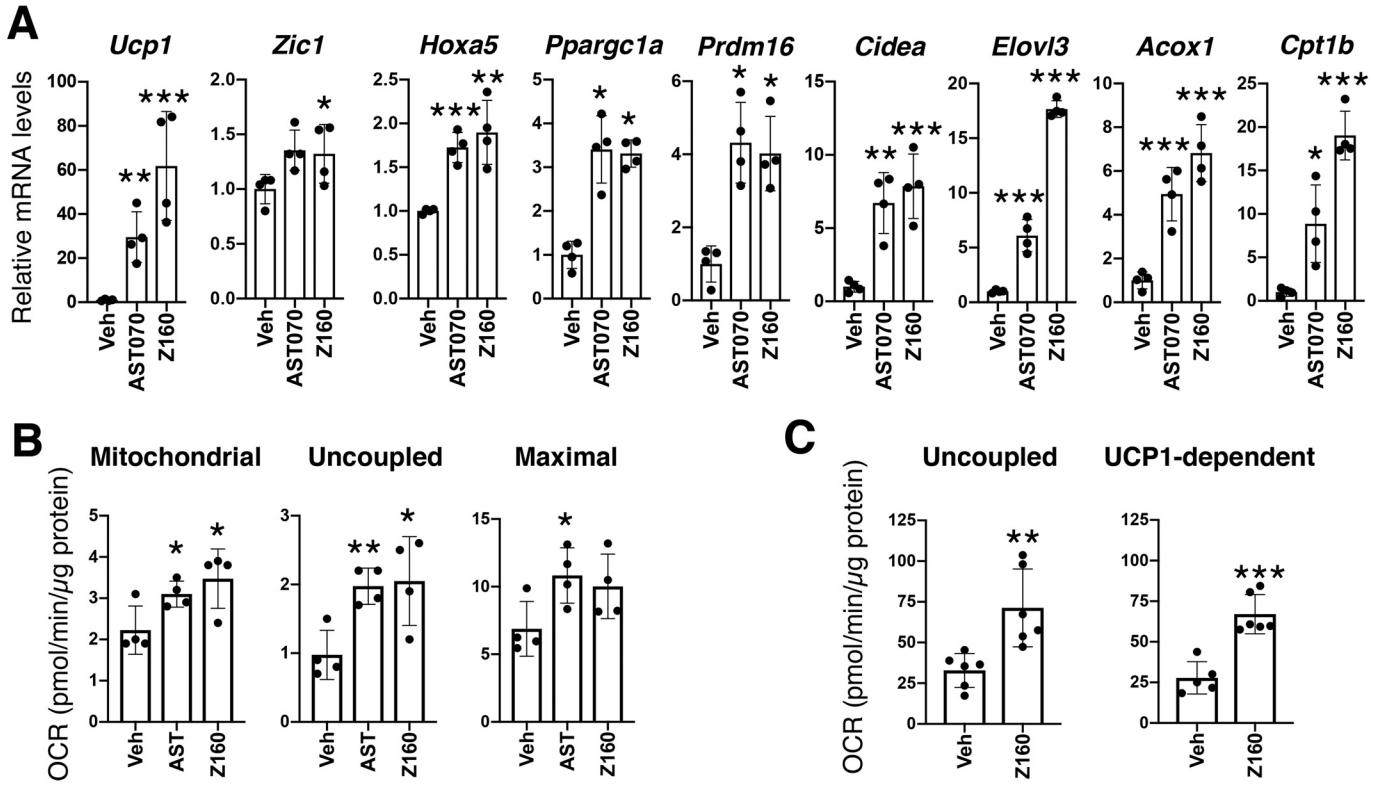

Figure 2. AST070 and Z160 activate thermogenic gene expression and mitochondrial activity in mouse brown adipocytes. *A*, relative expression of brown adipocyte, mitochondrial, and fatty acid oxidation markers after treatment with vehicle (*Veh*) or 10 μM AST070 or Z160 in primary brown adipocytes ($n = 4$). *B*, cellular respiration in immortalized brown adipocytes treated with vehicle or 10 μM AST070 or Z160 ($n = 4$). *C*, respiration from isolated mitochondria after vehicle or 10 μM Z160 treatment in immortalized brown adipocytes. UCP1-dependent respiration was obtained with 1 mM GDP ($n = 6$). All data presented as mean ± S.D. *, $p < 0.05$; **, $p < 0.01$; ***, $p < 0.001$.

mitochondrial respiration in mouse brown adipocytes as well as in human brown and white adipocytes.

Global gene expression analysis highlights Z160 effects on energy metabolism

To assess the effects of Z160 on global transcription in mouse brown adipocytes, we performed microarray analysis of RNA isolated from immortalized brown adipocytes treated with either vehicle or Z160. Compared with vehicle-treated cells, 581 and 504 probes were up-regulated and down-regulated, respectively, by at least 1.5-fold (Table S2). Consistent with our qPCR results, *Ucp1* was increased 2.5-fold in response to Z160, placing it in the top 20 up-regulated genes. We performed functional annotation of the genes up-regulated or down-regulated >1.5-fold by Z160 using the DAVID functional annotation tool (34). Z160 treatment increased expression of genes in mitochondrial categories (Fig. 4*A*), and down-regulated expression of genes that are distinct from mitochondrial function (Fig. 4*B*). In addition to *Ucp1*, up-regulated genes included five belonging to mitochondrial complex I (*Ndufb2*, *Ndufb4*, *Ndufb5*, *Ndufb9*, and *Ndufab1*), one associated with complex II (*Sdhd*) as well as cytochrome *c* (*Cycs*), two subunits of complex IV (*Cox6a2* and *Cox7b*), and two of complex V (*Atp5a1*, *Atp5e*). We confirmed results of the microarray using qPCR for representative genes from each electron transport chain complex (Fig. 4*C*). A slight enhancement in mitochondrial complex protein abundance was also observed in isolated mitochondria by Western blotting (Fig. 4*D*).

Z160 stimulates thermogenesis in the mouse

We assessed the ability of Z160 to stimulate thermogenesis *in vivo* in C57BL/J mice. A single subcutaneous injection of the drug led to an increase in body temperature 24 h later by 0.8 °C (37.5 *versus* 38.3 °C, $p < 0.05$), consistent with activated thermogenesis (Fig. 5*A*). Additionally, BAT from treated mice had elevated *Ucp1* mRNA and protein levels, and enhanced expression of several genes implicated in mitochondrial function and lipolysis (Fig. 5, *B* and *C*). No liver toxicity was observed as assessed by circulating aspartate aminotransferase (AST) levels (Fig. 5*D*). Plasma glucose levels were not affected by Z160 (172.8 ± 26.0 *versus* 157.6 ± 26.2 mg/dl, for vehicle- and Z160-treated mice, respectively).

Z160 activates PKA

To understand the mechanism by which Z160 and related compounds enhance mitochondrial respiration, we treated brown adipocytes with Z160 in the presence of several known antagonists in the adrenergic receptor signaling pathway. Treatment with vehicle or nonselective α-tolazoline (Tola) and β-propranolol (Prop) adrenergic receptor antagonists did not prevent the induction of *Ucp1* mRNA by Z160 (Fig. 6*A*). The same result was obtained with β3-adrenergic receptor antagonists (SR59230A, SR). By contrast, treatment with antagonists

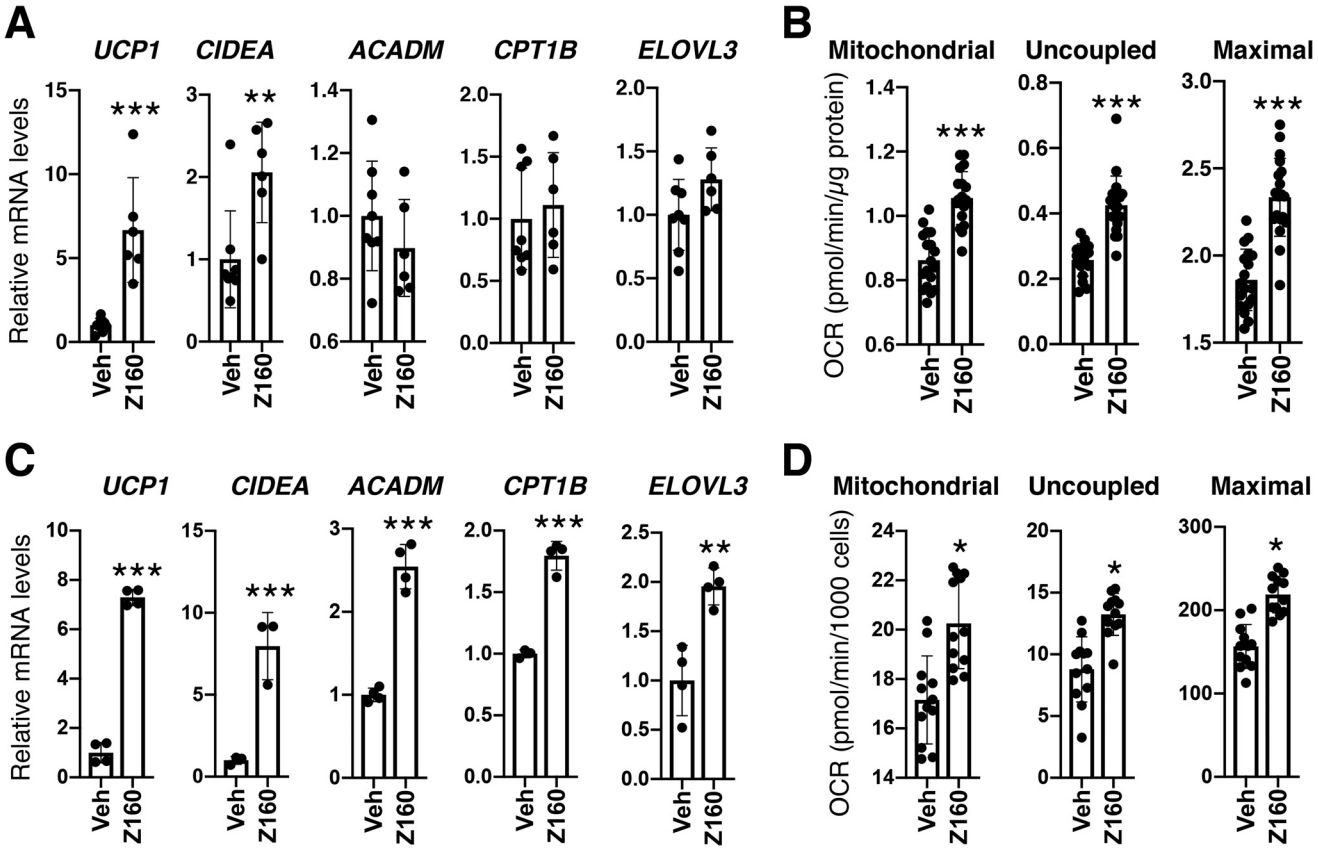

Figure 3. Z160 activates thermogenic gene expression and mitochondrial activity in immortalized human brown and white adipocytes. Cells were treated with vehicle (*Veh*) or 10 μM Z160 for 4 days. Relative expression of brown adipocyte, mitochondrial, and fatty acid oxidation markers in human brown (*A*) and white (*C*) adipocytes (n = 6-8 and n = 4 for brown and white adipocytes, respectively) and cellular respiration in human brown (*B*) and white (*D*) adipocytes (n = 20 and n = 12 for brown and white adipocytes, respectively). All data presented as mean ± S.D. *, $p < 0.05$; **, $p < 0.01$; ***, $p < 0.001$.

of PKA (H-89) or p38 MAPK (SB202190, SB) blocked the effect of Z160, suggesting that Z160 requires PKA activity to exert its effect on *Ucp1* expression. Accordingly, the Z160 enhancement of *Cidea* and *Elovl3* expression was also blunted by treatment with H-89 (Fig. 6*B*).

Based on these findings, we tested whether the AST070 or Z160 compounds influence PKA activity using a solid phase ELISA. First, we measured PKA activity in lysates from immortalized brown adipocytes after 30 min treatment with 50 μM AST070 or Z160. Treatment with either compound significantly increased PKA activity in an expected range (35, 36) (Fig. 6*C*). Next, we treated lysate with different Z160 concentrations. Z160 concentration as low as 25 μM showed a significant increase in PKA activity (Fig. 6*D*). Importantly, 25 μM Z160 also stimulated PKA activation in mouse BAT or liver extracts (Fig. 6*E*). To confirm the results, we treated cell lysates for 10 min with PKA antagonist H-89 (500 μM) followed by 30 min incubation with Z160 (50 μM). Preincubation with the PKA antagonist reduced the PKA activity and negated the Z160 response (Fig. 6*F*).

Z160 promotes p38 MAPK phosphorylation and lipolysis

The demonstration that Z160 influences PKA activity prompted us to investigate its effects on pathways downstream of PKA activation. In adipocytes, PKA indirectly activates p38 MAPK and promotes lipolysis (37, 38). Thus, the Z160-induced PKA activation was further characterized by first analyzing p38 MAPK phosphorylation. As depicted in Fig. 7*A*, Z160 caused p38 MAPK phosphorylation to a similar level as CL316,243. Additionally, Z160 induced lipolysis in brown adipocytes (Fig. 7*B*), and increased expression of lipolytic enzymes (adipose triglyceride lipase, *Atgl*; hormone-sensitive lipase, *Hsl*) and *FGF21* (a lipolytic mediator) at the mRNA level in both immortalized (Fig. 7*C*) and primary brown adipocytes (Fig. 7*D*).

Z160 modifies AKAP protein conformation and the mitochondrial PKA/AKAP interaction in brown adipocytes

Our data showing an effect of Z160 on PKA activity when added to cellular extracts (*e.g.* Fig. 6, *D* and *E*) suggested an effect of the compound directly on PKA or functionally associated proteins. The PKA tetramer consists of two catalytic and two regulatory subunits. In the mouse, these are catalytic subunits C-α and C-β, and regulatory subunits RI and RII, each with α and β isoforms (RI-α, RI-β, RII-α, and RII-β). PKA is also bound to a family of anchoring proteins, AKAPs, which allow the compartmentalization of cAMP signaling. To investigate whether Z160 binds PKA complex proteins, we applied two techniques that rely on ligand-induced alterations in protein stability: cellular thermal shift assay (CETSA) and drug affinity responsive target stability (DARTS). CETSA is based on the principle that ligand binding will change the temperature at which a protein starts to unfold and aggregate (39), whereas

A

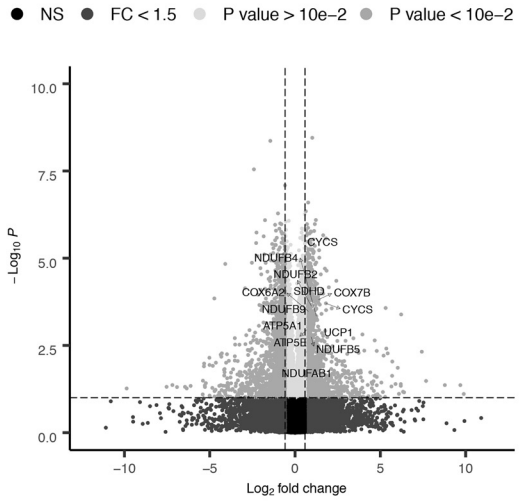

B

GO Cellular component up

Term	Genes	Benjamini
Mitochondrion	88	1.1E-10
Mitochondrial inner membrane	27	1.4E-4

GO Cellular component down

Term	Genes	Benjamini
Extracellular exosome	119	4.2E-14
Proteinaceous extracellular matrix	35	5.3E-13
Extracellular matrix	33	1.7E-12
Extracellular region	86	3.6E-12
Cell surface	45	9.2E-11
Extracellular space	72	1.6E-9
Basement membrane	17	6.8E-9
Focal adhesion	25	9.5E-5
Cytoplasm	178	4.7E-4

C

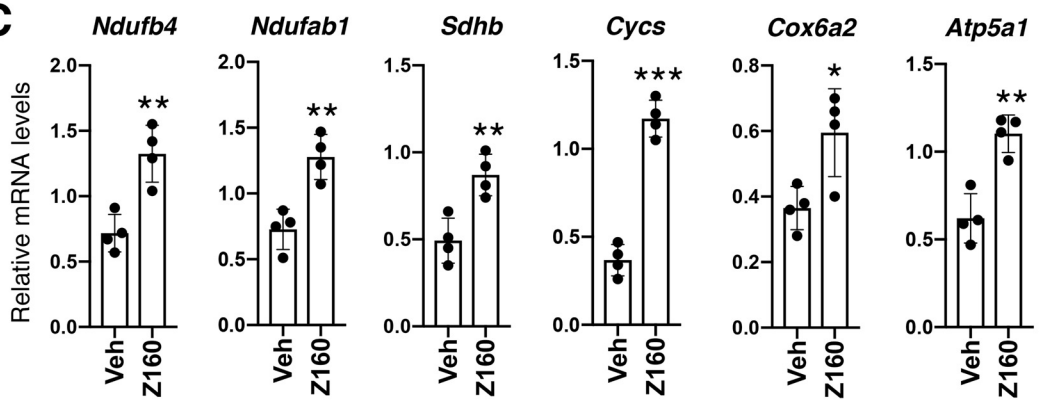

D

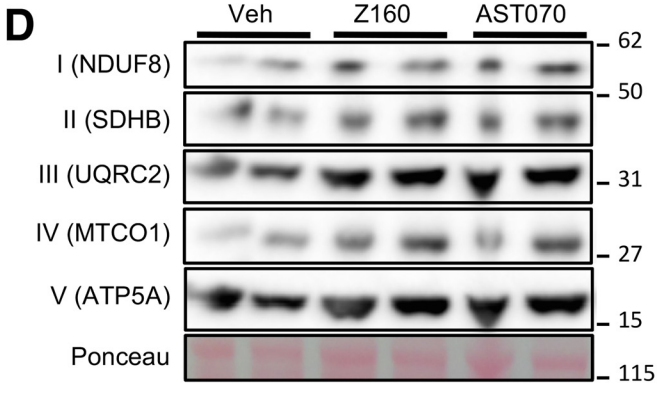

	Z160	AST070
I (NDUF8)	1.8x	1.9x
II (SDHB)	1.4x	1.3x
III (UQRC2)	1.5x	1.5x
IV (MTCO1)	1.9x	1.7x
V (ATP5A)	1.2x	1.2x

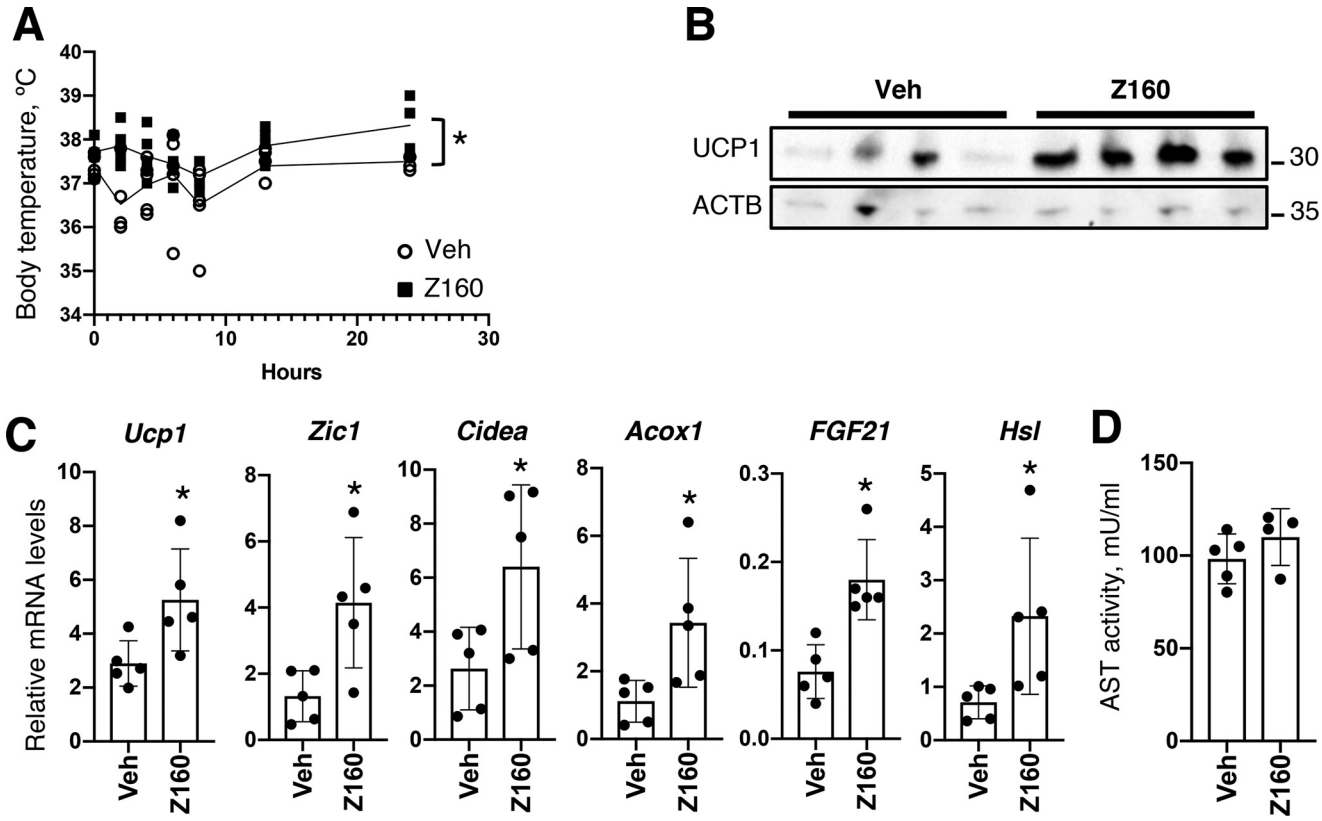

Figure 5. Z160 increases body temperature and mitochondrial gene expression in mouse BAT. Z160 at 1.5 mg/kg body weight was injected subcutaneously. Results were analyzed 20 h later. *A*, body temperature ($p < 0.05$ by two-way analysis of variance). *B*, UCP1 protein in BAT. β-ACTIN (*ACTB*) is a loading control. *C*, mRNA levels in BAT ($n = 5$). *D*, aspartate aminotransferase activity measured in plasma ($n = 4$-5). All data presented as mean ± S.D ($n = 5$). *, $p < 0.05$; **, $p < 0.01$.

DARTS relies on the protection of a protein from proteolysis upon specific binding to a small molecule (40).

We examined the potential interaction of Z160 with PKA subunits and AKAPs. First, we identified which PKA subunits and AKAP isoforms are normally present in BAT. Robust protein levels were observed in BAT for PKA C-α and RII-β subunits, AKAP1, and AKAP6 (also known as mAKAP) (Fig. 8*A*). To perform the CETSA assays, we incubated cultured brown adipocytes with 10 μM Z160 for 8 h, then analyzed the thermal shift by Western blotting. The PKA subunits expressed in BAT (C-α and RII-β) did not show differences in denaturation in the presence of Z160 (Fig. 8*B*). However, AKAP1 showed altered protein stability in the presence of Z160: Z160 increased the heat stability of AKAP1 (compare vehicle and Z160 heated at 55.8-63.3 °C), suggesting that Z160 may interact with this protein (Fig. 8*B*). By contrast, Z160 did not influence the heat stability of AKAP6, p38 MAPK, or cGMP-dependent kinase 1 (PKG-1).

To provide further evidence for an interaction between Z160 and AKAP1, we performed DARTS assays. Lysates from brown fat were treated with different Z160 concentrations for 1 h followed by Pronase digestion and immunoblotting. Representative data shown in Fig. 8*C* indicate that the presence of Z160 altered Pronase susceptibility of AKAP1 (compare with and without Z160 at a Pronase concentration of 1:4000). The protease susceptibility of other proteins tested was not influenced by the presence of Z160. The effect of Z160 on AKAP1 was confirmed using mouse brown adipocyte extracts (Fig. S4*A*). Importantly, the effect of AST070 or Z160 on AKAP1 was not observed with CL316,243, a chemically unrelated agent known to stimulate *Ucp1* expression (Fig. S4*B*).

AKAP1 is known to localize PKA to the surface of mitochondria and to relay cAMP signaling for mitochondrial functions (41, 42). We wondered whether treatment with our compounds could alter the binding of AKAP1 to mitochondria. To answer this question, we treated brown adipocytes with Z160 and isolated mitochondria at different times. In the presence Z160, AKAP1 protein levels were increased in the mitochondrial fraction after 6–8 h, suggesting that it may influence the localization of AKAP1 (Fig. 8*D*). In parallel, PKA subunits showed increased mitochondrial association after 6–8 h of Z160 treatment. By contrast, the levels of CYTC and GAPDH in the

Figure 4. Categories of genes regulated by Z160 in mouse-immortalized brown adipocytes. Global gene expression analysis was performed by microarray hybridization of RNA from brown adipocytes treated with vehicle or Z160. Genes with >1.5-fold alterations in gene expression in response to Z160 were identified and subjected to functional enrichment analysis (DAVID) using the GOTERM cellular component categories. The number of genes for each term, and multiple testing correction (Benjamini $p < 0.001$) are presented. *A*, volcano plot. *NS*, nonsignificant; *FC*, fold-change. *B*, categories showing up- and down-regulation by Z160. *C*, qPCR validation of microarray data for representative genes up-regulated by Z160 ($n = 4$). *D*, electron transport chain protein complexes detected by Western blotting in isolated mitochondria. Cells were treated overnight with vehicle (*Veh*), 10 μM Z160, or 10 μM AST070. Ponceau staining represents a loading control. Quantification as fold-change is presented on the right. All data presented as mean ± S.D. *, $p < 0.05$; **, $p < 0.01$; ***, $p < 0.001$.

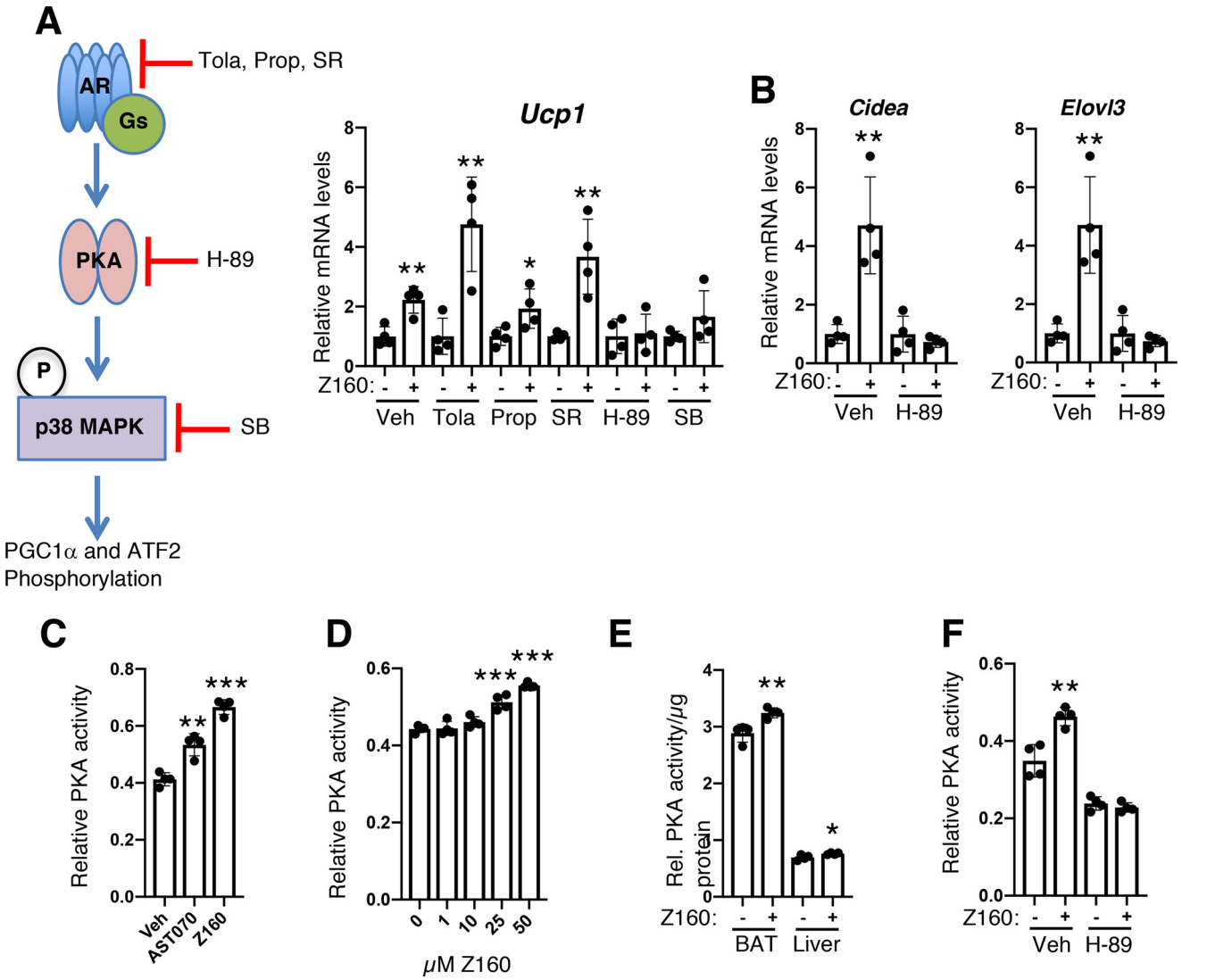

Figure 6. Z160 activates PKA. *A*, *Ucp1* mRNA levels in mouse immortalized brown adipocytes treated with 10 μM Z160 (+) and either vehicle (*Veh*) or 20 μM tolazoline (*Tola*), 20 μM propranolol (*Prop*), 20 μM SR59230A (*SR*), 20 μM H-89, 20 μM SB202190 (*SB*). Cells were treated with the inhibitors 1 h prior to and during overnight Z160 treatment. The schematic on the *left* shows where the inhibitors act on the adrenergic signaling pathway leading to increase of the Ucp1 expression. *B*, *Cidea* and *Elovl3* mRNA levels after 10 μM Z160 treatment (+) and in the presence of vehicle (Veh) or 20 μM H-89. H-89 was added 1 h prior and during the overnight Z160 treatment. *C*, PKA activity in immortalized brown adipocytes lysates treated 30 min with vehicle, or 50 μM AST070 or Z160. *D*, PKA activity in immortalized brown adipocyte lysates treated 30 min with Z160 concentrations are indicated. *E*, relative (*Rel.*) PKA activity in mouse tissue lysates treated 30 min with 25 μM Z160. *F*, PKA activity in immortalized brown adipocyte lysates treated with 50 μM Z160, in the presence of vehicle or 500 μM H-89. H-89 was added to the lysates 10 min prior the 30-min incubation with Z160. All data presented as mean ± S.D. ($n = 4$). *, $p < 0.05$; **, $p < 0.01$; ***, $p < 0.001$.

mitochondrial fraction were not altered by the compound. Total AKAP1 protein levels were not augmented by Z160, suggesting that the increased AKAP1 levels on mitochondria following treatment is due to AKAP1 translocation rather than an increase in protein synthesis (Fig. 8*E*). Finally, we assessed whether Z160 enhances interaction between AKAP1 and PKA subunits, a mechanism that may promote the localization of PKA at mitochondria. Brown adipocytes were treated with Z160 or AST070 for 7 h and cell lysates were precipitated by anti-AKAP1 antibody and immunoblotted with anti-PKA C-α and RII-β (Fig. 8*E*). The signal for PKA subunit precipitation by AKAP1 was slightly enhanced after treatment, especially with Z160, suggesting that the compounds increase the interaction between AKAP1 and the PKA subunits.

To further assess the requirement of AKAP1 to mediate the effects of Z160, we inactivated AKAP1 in an immortalized brown adipocyte cell line (AKAP1wt) using CRISPR/Cas9 gene editing. One clone (AKAP1mut) was selected based on very low AKAP1 protein levels (Fig. 9*A*). Unlike AKAP1wt cells, treatment of AKAP1mut cells did not respond to Z160 with increased *Ucp1* expression (Fig. 9*B*). Additionally, the Z160-induced gene expression was blunted or reduced in AKAP1mut for *Hoxa5*, *Cidea*, *Elovl3*, *Acox1*, and *Cpt1b*. However, Z160 increased *Ppargc1a* expression in both AKAP1wt and AKAP1-mut cells, suggesting that Z160 may exert some effects that are AKAP1-dependent, and others that are AKAP1-independent. Finally, we treated brown adipocytes with Z160 before assessing mitochondrial respiration. Z160 increased mitochondrial

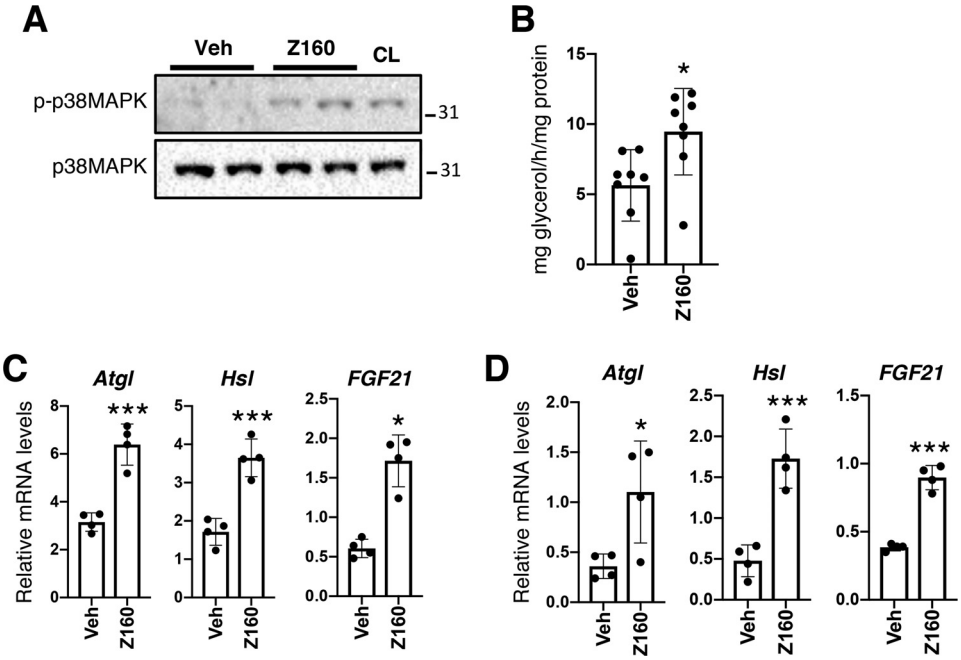

Figure 7. Z160 promotes p38 MAPK phosphorylation and lipolysis. *A*, Western blotting analysis of phosphorylated and total p38 MAPK protein. Immortalized brown adipocytes were treated overnight with vehicle (*Veh*), 10 μM Z160, or 10 nM CL316,243 (*CL*). *B*, lipolysis of endogenous lipid in immortalized brown adipocytes after 10 μM Z160 overnight treatment ($n = 8$). mRNA levels of lipolysis-related genes in immortalized (*C*) and primary (*D*) brown adipocytes measured by qPCR after 10 μM Z160 overnight treatment ($n = 4$). All data presented as mean ± S.D. *, $p < 0.05$; ***, $p < 0.001$.

and uncoupled respiration in AKAP1wt but not in AKAP1mut cells (Fig. 9*C*). In contrast, Z160-induced maximal respiration was significantly elevated in AKAP1mut cells. To confirm that the increase in uncoupled respiration was due to UCP1, we isolated mitochondria from cells treated with Z160. Uncoupled and UCP1-dependent respiration were significantly increased by Z160 in AKAP1wt but not in AKAP1mut mitochondria (Fig. 9*D*).

Discussion

In the present study, we identified a new compound family with the ability to increase mitochondrial respiration in mouse brown adipocytes and human white adipocytes. Furthermore, *in vivo* administration led to increased mitochondrial activity and thermogenesis. The compounds influenced the expression of many genes involved in mitochondrial and fat oxidation processes (*e.g. Ppargc1a*, *Cpt1b*, *Elovl3*, *Cidea*, and *Acox1*), indicating that Z160 may influence energy utilization through means that are UCP1-independent. Indeed, we identified PKA activation as a mechanism of action of these compounds, with particular effects on AKAP proteins and subcellular localization of PKA (Fig. 10). Our results highlight AKAP1 as a potential novel target for increasing cellular energy expenditure.

PKA is a key node in the β-adrenergic signaling pathway, controlling many cellular processes, including gene expression, lipolysis, and lipogenesis. It is thought that upon binding of cAMP to the two regulatory subunits of the PKA heterotetramer, the catalytic subunits of PKA are released and activated. Our findings are consistent with an effect of Z160 and related compounds on PKA activation, as they caused increased p38 MAPK phosphorylation, enhanced lipolysis, and induction of *Ucp1* expression. A proportion of PKA within the cell is associated with mitochondria (43), and PKA can increase electron transport chain activity by direct phosphorylation of complexes I and IV (44, 45). AKAP1 and its splice variants localize to mitochondria and interact with type I and type II regulatory subunits of PKA. Our findings show that Z160 and AST070 increase the amount of AKAP1 in the mitochondrial fraction and increase PKA/AKAP protein interaction. Possible mechanisms include the compounds promoting the interaction of AKAP at the mitochondrial surface with PKA, or increased localization of PKA/AKAP complexes to the mitochondria. AKAP1 and the RII-β subunit of PKA colocalize in mitochondria of white adipocytes (46). Our tissue distribution analysis indicates that AKAP1 and the RII-β are both present at higher levels in BAT than WAT, consistent with a role in mitochondria-rich cells.

Our studies showed altered protein conformation of AKAP1 in the presence of Z160, suggesting a direct interaction between Z160 and AKAP1. Although it might be expected that binding of a compound to a protein will enhance stability, in the DARTS assays we observed increased protease sensitivity of AKAP1 in the presence of Z160. There are several possible explanations. For example, Z160 binding could disrupt the tridimensional structure of the AKAPs and make specific domains more accessible to protease digestion. The actual binding domain may still be stabilized by Z160, but not detectable with the specific antibody employed. It is also possible that Z160 binds another protein associated with the PKA/AKAP complex, and thereby modifies the protein complex to stimulate local PKA activity. As noted, our AKAP1mut brown adipocyte cell line attenuated several effects of Z160, including induction of several genes (*Cpt1b*, *Elovl3*, *Cidea*, *Acox1*, and *Ucp1*), as well as uncoupled respiration. However, AKAP1 was not required for Z160 effects on *Ppargc1a* expression, nor

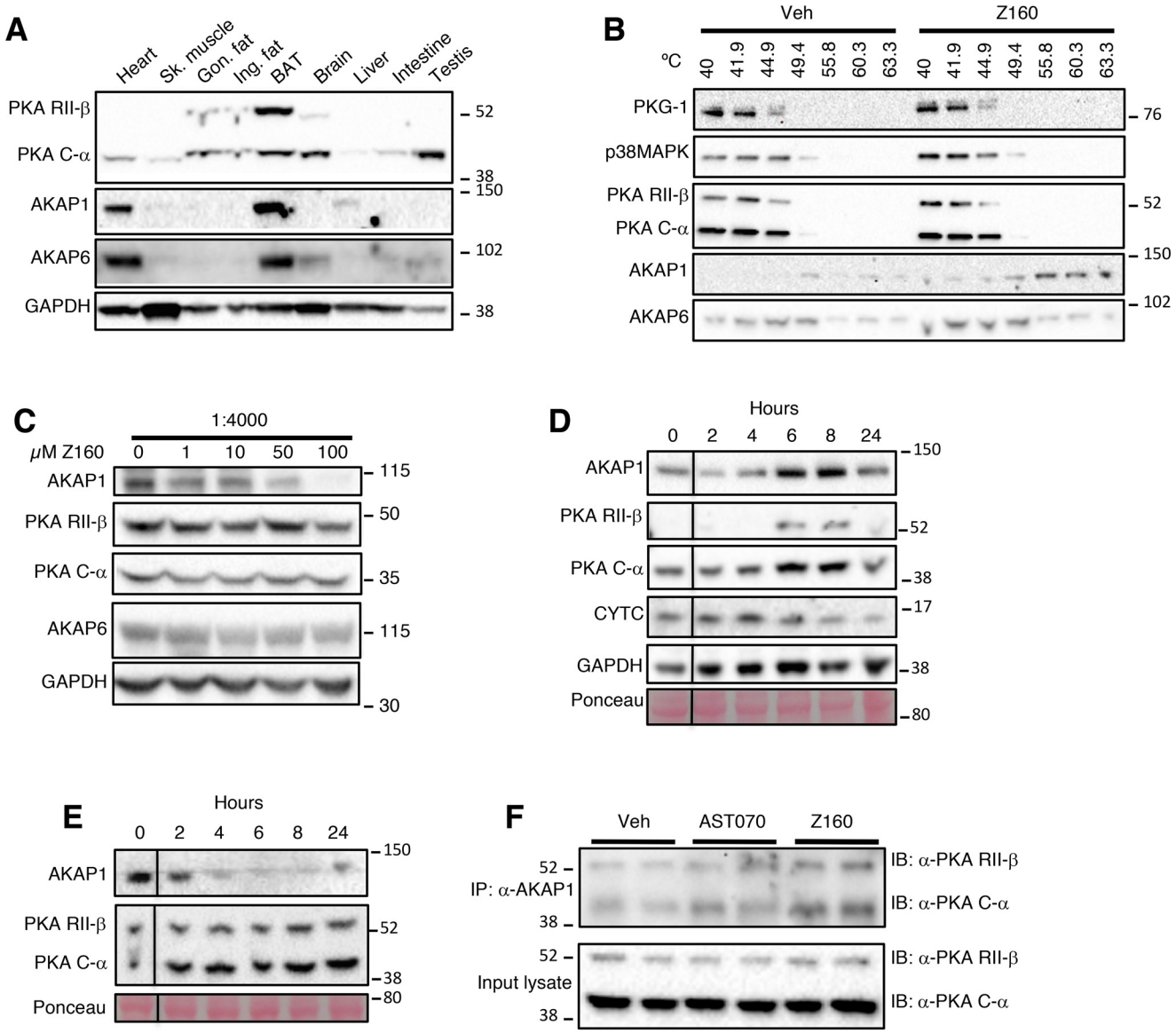

Figure 8. Z160 modifies AKAP protein conformation and localization in brown adipocytes. *A*, tissue distribution of PKA subunits and AKAPs in mouse tissues determined by Western blotting with the indicated antibodies. GAPDH represents a loading control. *Sk*, skeletal; *Gon*, gonadal; *Ing*, inguinal. *B*, representative Western blotting of a CETSA assay in immortalized brown adipocytes treated with vehicle (*Veh*) or 10 μM Z160 overnight. Temperature (°C) is indicated across the *top*. *C*, representative Western blotting of a DARTS assay in BAT extracts treated with different Z160 concentrations for 1 h. Pronase dilution is indicated across the *top*. *D*, Western blotting of mitochondria-associated proteins isolated from immortalized brown adipocytes treated with 10 μM Z160 for the indicated time. *E*, Western blotting of total proteins isolated from immortalized brown adipocytes treated with 10 μM Z160 for the indicated time. *F*, co-immunoprecipitation of PKA C-α and PKA RII-β with AKAP1. Immortalized brown adipocytes were treated with vehicle, 10 μM AST070, or 10 μM Z160 for 7 h.

maximal respiration. This suggests that AKAP1 is required for some, but not all, effects of Z160. Nevertheless, the two techniques used here (CETSA and DARTS) identified AKAP1 (and ruled out PKA subunits) as the best target. Future studies to identify Z160 targets using high-throughput approaches may shed additional light on this compound's mode of action.

The induction of thermogenesis is an appealing approach to influence energy expenditure and reduce obesity. Pharmacological agents that increase metabolic rate by increasing mitochondrial uncoupling (such as 2,4-dinitrophenol) have been dismissed for lack of tissue specificity and severe side effects (47). Targeting proteins downstream of PKA, such as p38 MAPK and PPARγ, has limitations due to pleiotropic effects (48–50). Therefore, there is a real need to identify new mechanisms to modulate this pathway (9). The AKAP proteins, which control the spatiotemporal activation of PKA in a tissue-dependent manner, may offer an alternative therapeutic target for promoting energy expenditure. AKAP1 is the most abundant AKAP in adipose tissue (51), and plays a role in mitochondrial-related PKA activity, as well as in lipoprotein lipase expression (25, 41). Furthermore, AKAP1 appears to be an amenable target to increase mitochondrial activity and lipolysis in both brown and white adipocytes, and makes it an attractive candidate for therapeutic applications related to obesity. Further studies will investigate whether the compounds can have a long-term effect on diet-induced obesity in mice. However, we acknowledge that modulation of AKAP1 and mitochondrial uncoupling may have unpredictable and detrimental effects in tissues other than

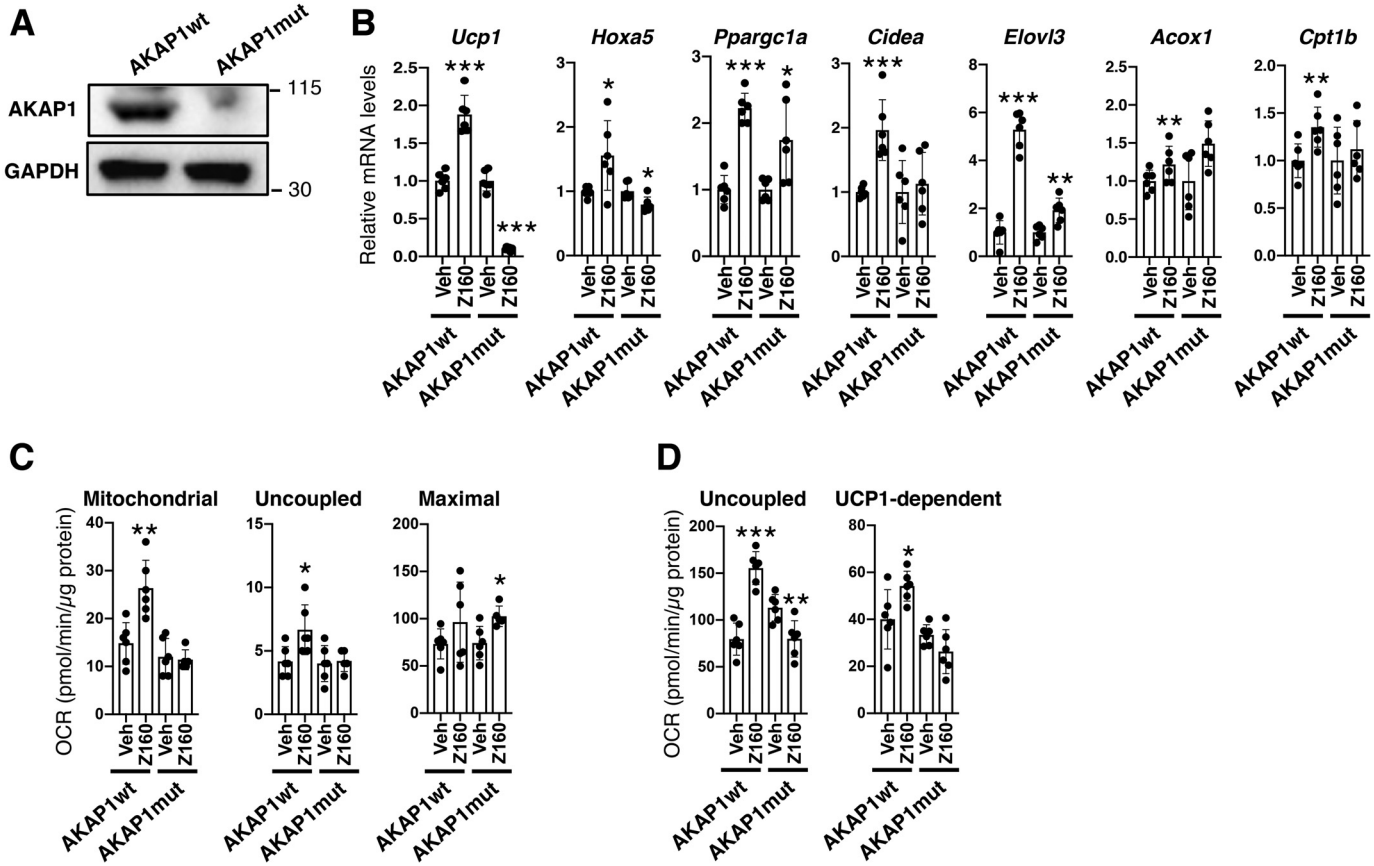

Figure 9. Generation and characterization of an AKAP1 mutant brown adipocyte cell line. *A*, cell lysates of the AKAP1wt and AKAP1mut cell lines probed with the AKAP1 antibody. GAPDH is a loading control. *B*, relative expression of brown adipocyte, mitochondrial, and fatty acid oxidation markers after treatment with vehicle (*Veh*) or 10 μM Z160. *C*, cellular respiration in immortalized brown adipocytes treated with vehicle or 10 μM Z160. *D*, respiration from isolated mitochondria after vehicle or 10 μM Z160 treatment in immortalized brown adipocytes. UCP1-dependent respiration was obtained with 1 mM GDP ($n = 6$); mean ± S.D. *, $p < 0.05$; **, $p < 0.01$; ***, $p < 0.001$.

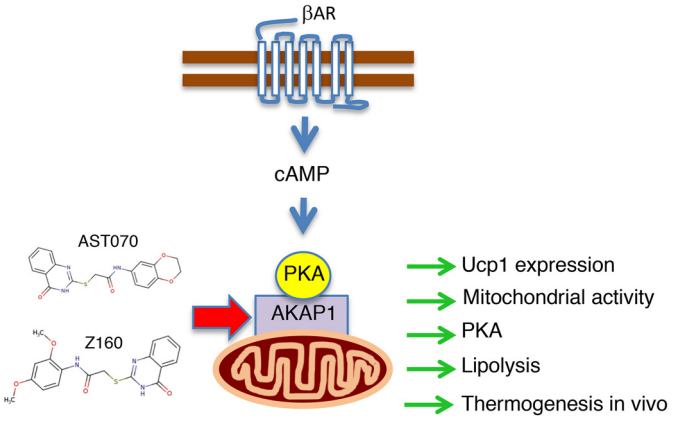

Figure 10. Schematic of the effects of AST070 and Z160. The compounds interact with and localize AKAP1 on mitochondria. The change in AKAP1/PKA subcellular localization seems to promote *Ucp1* expression, mitochondrial and PKA activity, as well as lipolysis in brown and white adipocytes.

brown adipose tissue, such as heart. Thus, further development for therapeutic applications would require evaluation of effects in other organs, and may require targeted delivery to brown adipose tissue.

In summary, we have identified new compounds with the ability to promote uncoupled respiration in mouse brown adipocytes and human white adipocytes, and to promote thermogenesis in the mouse. These compounds influence a broad range of gene expression related to mitochondrial respiration, and appear to exert some actions independently of UCP1. These include previously unexploited mechanisms of action that involved modulation of PKA/AKAP interactions and/or localization to mitochondria, which may overcome some limitations in existing compounds.

Experimental procedures

Cell culture

Primary brown adipocytes were isolated as described previously (52). An established mouse brown adipocyte cell line was obtained from Dr. Bruce Spiegelman (Dana-Farber Cancer Institute, Boston, MA, USA) (53). To differentiate primary and immortalized brown adipocytes, cells were grown until confluence in Dulbecco's modified Eagle's medium containing 10% fetal bovine serum, 25 mM glucose 1 mM pyruvate, 2 mM glutamine, 20 nM insulin, 1 nM triiodothyronine, and antibiotics (53). Once confluent (day 0), differentiation was induced by supplementing the medium with 0.5 mM isobutylmethylxanthine (IBMX), 0.5 μM dexamethasone, and 0.125 mM indomethacin, for 2 days. Differentiation was continued in the original medium (without IBMX, dexamethasone, and indomethacin) for 7-10 days.

Human-immortalized brown and white preadipocytes were obtained from Dr. Yu-Hua Tseng (Joslin Diabetes Center, Harvard Medical School, USA). The generation of the two cell lines from human neck adipose tissue biopsies and immortalization was performed as previously described (54) but from a different donor. Cells were cultured in high glucose Dulbecco's modified Eagle's medium supplemented with 10% fetal bovine serum and antibiotics. 2 days after reaching confluence, cells were treated with 30 μM biotin, 500 nM insulin, 17 μM pantothenate, 100 nM dexamethasone, 2 nM 3,3',5-triiodo-L-thyronine, 500 μM IBMX, 30 μM indomethacin, and 1 μM rosiglitazone, for 12 days. Afterward, cells were treated with 30 μM biotin, 500 nM insulin, 17 μM pantothenate, and 2 nM 3,3',5-triiodo-L-thyronine (maintenance media) for 2 days with end point assays were performed on day 18, and for 5 days with end point assays were performed on day 21, for the brown and white adipocytes cells, respectively.

Generation of brown adipocyte UCP1-reporter cell lines

Different lengths of mouse *Ucp1* promoter were cloned into pGL3-basic vector (Promega) by PCR, using the NheI and XhoI sites. We PCR-amplified *Ucp1* promoter fragments of 2.3 (cttgatgtgtggagctgagtagc), 3 (gtgccgtcactaacagtactg, 5 (ctgcagactcctgacacagct), and 7 kb (ggaaagtggttcagtttgattagaagg) plus 94 bases downstream of the transcription start site (reverse primer: ctaggtagtgccagtgcagag). To perform chemical library screening in mature brown adipocytes, we created stable cell lines in the immortalized mouse brown adipocytes (53). For this purpose, we introduced a neomycin cassette from pcDNA3.1/V5-His vector (Invitrogen) into the SalI site of pGL3-basic plasmid. All constructs were verified by sequencing. Stable cell lines were selected with 500 μg/ml of G418.

Luciferase assay for pilot studies prior to drug screen

Stable brown adipocyte cell lines carrying *Ucp1* promoter–luciferase constructs were seeded in 96-well–plates and differentiated for 7–10 days. Cells were treated with either 10 nM CL316,243, 10 μM forskolin, 1 μM rosiglitazone, or 1 μM cis- and trans-retinoic acid, overnight. Luciferase activity was assayed using LAR II or Bright-Glo luciferase assay system (Promega). For the LAR II assays, passive lysis was performed on the cells. Luminescence was measured with a GloMax Luminometer. We did not notice differences in response between LAR II and Bright-Glo and the latter was used for the drug screen.

Small molecule library screen

The screen was conducted at the UCLA Molecular Screening Shared Resource using automated instruments. Immortalized brown adipocytes were differentiated in T225 flasks and plated in Matrix 384-well–plates (26,000 cells per well) with white flat bottoms (ThermoScientific) using trypsin and collagenase type II (Sigma, C6885). The small molecule libraries screened were a BioMol library (204 compounds), an FDA-approved drug library (1120 compounds), a Microsource spectrum collection (2000 compounds), and a druggable compound set (8000 compounds). Molecules were delivered at 10 μM final concentration in DMSO. The screen was performed in duplicate on different days. After 18 h, luciferase activity was measured with Bright-Glo luciferase assay system and an LJL instrument. Data were normalized to the basal response (100% activity) in the presence of DMSO. Following the primary screen, 92 molecules were selected for validation and used to treat brown adipocyte cells plated in a 96-well–plate overnight. RNA was extracted with an SV 96 Total RNA Isolation System (Promega). Compounds used for follow-up studies were identified using search tools available from Molport, and ordered from the same company.

Cellular bioenergetics

Cellular respiration was measured using a Seahorse XF24 or XF96 analyzer (Agilent), as previously published (55). Immortalized brown adipocytes were differentiated in 6-well–plates and replated in the XF24 plates at a density of 50,000 cells/well using trypsin and collagenase type II. Cells were treated with vehicle (DMSO) or compounds for 18–24 h. Oxygen consumption rates were obtained before and after the sequential injection of 0.75 μM oligomycin, 0.5 μM FCCP, and 0.75 μM rotenone/myxothiazol. Results were normalized to total protein. For human white adipocytes, cells were cultured as described above and differentiated in XF96 microplates. DMSO or Z160 (10 μM) were added at day 17 for 4 days. Oxygen consumption rates were measured before and after the sequential injection of 1 μM oligomycin, 1 μM FCCP, and 0.5 μM rotenone/antimycin A. For these cells, results were normalized to cell count determined by nuclei fluorescent staining with Hoescht staining imaged on a Cytation 5 Imaging Reader and analysis with Gen5 software (BioTek). Respiration from isolated mitochondria were performed with 10 mM succinate as described previously (56, 57). Oxygen consumption rates were obtained before and after the sequential injections of 2.5 μM oligomycin and 1.5 μg/ml of antimycin A. UCP1-dependent respiration was measured by injecting 1 mM GDP and represents the GDP-sensitive respiration. For both mouse and human cell lines, mitochondrial respiration was calculated by subtracting the non mitochondrial respiration present after the last injection (rotenone/myxothiazol or rotenone/antimycin A). Uncoupled respiration corresponds to the respiration difference between oligomycin and the last injection. Maximal respiration was determined after FCCP injection.

Gene expression analysis

Mouse RNA levels were measured by qPCR as described previously (56). Data were normalized to *B2m* and *Tbp* reference genes. Primers are listed in Table S3. Human RNA was extracted using an RNA Mini Plus kit (Zymo) and gene expression determined by TaqMan assay. The one-step qPCR was run on a QuantStudio 12K Flex Real Time PCR System (ThermoFisher) using the following protocol: 50 °C for 5 min, 95 °C for 20 s, 40 cycles of 95 °C for 15 s, and 60 °C for 60 s. Data were normalized to *PPIA* and *PSMB2* reference genes. TaqMan probes (ThermoFisher Scientific) are listed in Table S3. For global gene expression analysis, RNA isolated from brown adipocytes treated with compounds as indicated (four biological

replicates) was hybridized to Illumina mouse Ref 8 V2.0 bead chips at the University of California, Los Angeles Neuroscience Genomics Core as previously described (56). Data were processed with GenomeStudio V2011.1 using the quantile normalization, background subtraction, and a present call of $p < 0.05$.

Immunoblot analysis

Cells and tissues were lysed in 10 mM Tris, pH 7.5, 10 mM NaCl, 1 mM EDTA, and 0.5% Triton X-100, supplemented with complete mini EDTA-free protease (Roche Diagnostics) and phosphatase (mixtures 2 and 3, Sigma) inhibitors, followed by a 10-s sonication. For analysis of mitochondrial proteins, mitochondria were isolated from cells by dual centrifugation, as described (57). Protein lysates were separated by SDS-PAGE and transferred to a nitrocellulose membrane. Transfer was confirmed by Ponceau staining (P7170, Sigma). After blocking in 5% milk, 0.1% Tween-20 in Tris-buffered saline, primary antibody was incubated overnight at 4 °C in 5% BSA and 0.1% Tween-20 in Tris-buffered saline. Primary antibodies against ACTB (GTX109639, lot 42606, GeneTex), AKAP1 (5203, lot 1, Cell Signaling), AKAP6 (07-087, lot 2926062, Millipore), cytochrome *c* (136F3, lot 3, Cell Signaling), electron transport chain protein complexes (Total OXPHOS rodent WB antibody mixture ab110413, Abcam), GAPDH (GTX100118, lot 43712, Genetex), active p38 MAPK (V1211, lot 23053205, Promega), total p38 MAPK (8690, lot 3, Cell Signaling), PGC1α (AB3242, lot 2181243, Millipore), phospho-(Ser/Thr) PKA substrate (9621, Cell Signaling), PKA C-α (4782, lot 3, Cell Signaling), PKA RII-β (ab75993, lot GR90233-8, Abcam), and UCP1 (662045, lot D00076504, Calbiochem) were used at 1:2000. Peroxidase goat anti-rabbit (sc-2030, Santa Cruz Biotechnology, Inc.) or rabbit anti-mouse (A9044, lot 115K4811, Sigma) secondary antibody was used at a 1:10,000 dilution for 1 h at room temperature in 5% milk and 0.1% Tween-20 in Tris-buffered saline. Immunoreactive bands were revealed with ECL prime (Amersham Biosciences) and visualized with a Bio-Rad Gel-doc imager. Quantification using representative bands from the Ponceau staining was performed with ImageJ (58).

Co-immunoprecipitation

Immortalized brown adipocyte cells were differentiated for 10 days and treated with 10 μM AST070 or Z160 for 7 h. Cells were lysed in 150 mM NaCl, 50 mM Tris, pH 7.5, 1% Nonidet P-40, 0.5% sodium deoxycholate containing protease and phosphatase inhibitors. Cell lysates were incubated overnight at 4 °C with 2 µl of anti-AKAP1 antibody. Twenty microliters of Protein A/G PLUS-agarose beads (Santa Cruz Biotechnologies) were added for 2 h at 4 °C. After an initial wash (500 mM NaCl, 50 mM Tris, pH 7.5, 0.1% Nonidet P-40, 0.05% sodium deoxycholate), and a final wash (10 mM Tris, pH 7.5, 0.1% Nonidet P-40, 0.05% sodium deoxycholate), proteins were eluted from the beads with 1× loading buffer and 2% β-mercaptoethanol, boiled for 10 min, and analyzed by Western blotting. To avoid detecting the IgG heavy chain, TidyBlot Western blotting reagent:horseradish peroxidase (Bio-Rad) at 1:100 was used as secondary antibody to reveal the PKA subunits from the co-immunoprecipitation blot.

Assessment of PKA activity

PKA kinase activity was measured with an ELISA that utilizes a synthetic peptide as substrate for PKA and a polyclonal antibody that recognizes the phosphorylated form of the substrate (ab139435, Abcam). PKA activity was measured in lysates from cultured brown adipocytes, mouse BAT, or liver. Cells and tissues were lysed in 20 mM MOPS, 5 mM EGTA, 2 mM EDTA, and 0.1% Triton X-100 supplemented with protease and phosphatase inhibitor as described above. Protein concentration was determined by a Bradford assay and 10 µg of cells, 0.25 µg of BAT extract, or 0.5 µg of liver extract were assessed for PKA activation according to the manufacturer's instructions, with minor changes. Briefly, vehicle or Z160 were incubated with brown adipocyte cells overnight or with protein lysates for 30 min, followed by one wash before the primary antibody, 60 min incubation with the primary antibody, 30 min incubation with the secondary antibody, and by 10 min washing. Absorbance was measured after the substrate was added for 20-60 min depending on the intensity of the signal.

Lipolysis assay

Lipolysis was assessed in cultured cells using medium collected over 3 h with the Adipolysis assay kit (AB100, Millipore), according to the manufacturer's protocol.

CETSA

CETSA assays were performed as described (59). Briefly, differentiated brown adipocytes (one 10-cm dish per treatment) were treated with vehicle or compounds, trypsinized, counted, and resuspended in ~450 µl of PBS containing protease inhibitors (volumes were adjusted to have the same number of cells in each treatment). For each sample, 18 µl was distributed into each of 7 PCR tubes. Samples were heated using a thermocycler with a temperature gradient (iCycler, Bio-Rad) for 3 min, followed by 3 min at room temperature, and then snap-frozen in liquid N_2. After two freeze-thaw cycles, samples were centrifuged at 20,000 × *g* for 15 min at 4 °C, and the supernatants were transferred to another set of tubes. Proteins were analyzed by immunoblotting.

DARTS

DARTS assays were performed as described (40). Briefly, BAT or cells within a 10-cm dish were lysed with 600 µl of M-PER buffer containing protease and phosphatase inhibitors. Debris was pelleted by centrifugation at 18,000 × *g* for 10 min at 4 °C, and the lysates were harvested and supplemented with TNC buffer (50 mM Tris-HCl, 50 mM NaCl, 10 mM $CaCl_2$). The lysates were split into two tubes and treated with either vehicle or 20 μM Z160 for 1 h at room temperature. For the experiment with BAT, 100 µg of lysate was incubated with different Z160 concentrations. Different concentrations of Pronase (from 1:100 to 1:10,000 dilution from a 1.25 mg/ml of Pronase stock, number 10165921001, Roche) were incubated with the samples for 30 min at room temperature and the reaction was stopped with SDS loading

buffer followed immediately by heating at 70 °C for 10 min. Samples were analyzed by immunoblotting.

CRISPR/Cas9 Akap1 gene editing

Two gRNAs were selected using sgRNA Designer from the Broad Institute (gRNA1: gagggggcaagtaacccgag and gRNA2: actggctccacaaagctact). Cloning was performed using pSpCas9 (BB)-2A-puro (PX459) V2.0 vector (Addgene plasmid number 62988). Plasmid construction was confirmed by sequencing. A puromycin-sensitive brown adipocyte cell line (60) was transfected with the two plasmids and selected with 3 μg/μl of puromycin. Single-cell cloning was performed in a 96-well–plate and clones were selected by Western blotting to detect AKAP1 protein knockdown, and confirmed by sequencing after PCR amplification (PCR primers: gcaagagtcttcaagccccg and ggagaagaggtgagccatgg).

Animal experiments

All mouse studies were conducted in accordance with and approved by the Institutional Animal Research Committee of the University of California, Los Angeles. C57BL/6J male mice were obtained from the Jackson Laboratory. For the drug injection, Z160 (diluted in 100 μl DMSO) was injected subcutaneously, near BAT, at 1.5 mg/kg body weight and compared with vehicle alone. Plasma and tissues were obtained after 20 h. Body temperature was obtained with a rectal probe (BAT-12, Physitemp). AST activity was determined from plasma according to the manufacturer's protocol (MAK055, Sigma).

Statistical analyses

Statistical analyses were performed by unpaired two-tailed Student's *t* test. A value of $p < 0.05$ was considered significant.

Data availability

The microarray data are deposited in Gene Expression Omnibus (GSE138264). All remaining data are contained within the article.

Acknowledgments—We thank Brett Lomenick and Jing Huang for providing Pronase and helpful discussions about DARTS experiments. We thank Dr. Yu-Hua Tseng for the human adipocyte cell lines.

Author contributions—L. V. and K. R. conceptualization; L. V. data curation; L. V., J. Y. L., G. R. D., and C. D. C. formal analysis; L. V. and K. R. supervision; L. V., J. Y. L., G. R. D., and C. D. C. investigation; L. V. and G. R. D. methodology; L. V., C. D. C., and K. R. writing-original draft; L. V., J. Y. L., G. R. D., C. D. C., and K. R. writing-review and editing; K. R. funding acquisition.

Funding and additional information—This work was supported by Fondation Leducq Grant 12CVD04 and National Institutes of Health, NHLBI Grant P01 HL028481. The content is solely the responsibility of the authors and does not necessarily represent the official views of the National Institutes of Health.

Conflict of interest—The authors declare that they have no conflicts of interest with the contents of this article.

Abbreviations—The abbreviations used are: BAT, brown adipose tissue; WAT, white adipose tissue; UCP1, uncoupling protein-1; PKA, protein kinase A; AKAP, A kinase anchoring protein; DARTS, drug affinity responsive target stability; CETSA, cellular thermal shift assay; CRISPR, clustered regularly interspaced short palindromic repeats; ; AST, aspartate aminotransferase; MAPK, mitogen-activated protein kinase; qPCR, quantitation PCR; PPARγ, peroxisome proliferator-activated receptor γ; Tola, tolazoline; Prop, propranolol; IP, immunoprecipitation; IB, immunoblot; GAPDH, glyceraldehyde-3-phosphate dehydrogenase; IBMX, isobutylmethylxanthine; gRNA, guide RNA; FCCP, carbonyl cyanide p-trifluoromethoxyphenylhydrazone.

References

1. Twig, G., Yaniv, G., Levine, H., Leiba, A., Goldberger, N., Derazne, E., Ben-Ami Shor, D., Tzur, D., Afek, A., Shamiss, A., Haklai, Z., and Kark, J. D. (2016) Body-mass index in 2.3 million adolescents and cardiovascular death in adulthood. *N. Engl. J. Med.* **374,** 2430–2440 CrossRef Medline
2. Juonala, M., Magnussen, C. G., Berenson, G. S., Venn, A., Burns, T. L., Sabin, M. A., Srinivasan, S. R., Daniels, S. R., Davis, P. H., Chen, W., Sun, C., Cheung, M., Viikari, J. S. A., Dwyer, T., and Raitakari, O. T. (2011) Childhood adiposity, adult adiposity, and cardiovascular risk factors. *N. Engl. J. Med.* **365,** 1876–1885 CrossRef Medline
3. Galgani, J., and Ravussin, E. (2008) Energy metabolism, fuel selection and body weight regulation. *Int. J. Obes.* **32,** S109–S119 CrossRef
4. Hill, J. O., Wyatt, H. R., and Peters, J. C. (2012) Energy balance and obesity. *Circulation* **126,** 126–132 CrossRef Medline
5. Kajimura, S., and Saito, M. (2014) A new era in brown adipose tissue biology: molecular control of brown fat development and energy homeostasis. *Annu. Rev. Physiol.* **76,** 225–249 CrossRef Medline
6. Giordano, A., Frontini, A., and Cinti, S. (2016) Convertible visceral fat as a therapeutic target to curb obesity. *Nat. Rev. Drug Discov.* **15,** 405–424 CrossRef Medline
7. Wankhade, U. D., Shen, M., Yadav, H., and Thakali, K. M. (2016) Novel browning agents, mechanisms, and therapeutic potentials of brown adipose tissue. *Biomed. Res. Int.* **2016,** 2365609–2365615 CrossRef Medline
8. Betz, M. J., and Enerbäck, S. (2018) Targeting thermogenesis in brown fat and muscle to treat obesity and metabolic disease. *Nat. Rev. Endocrinol.* **14,** 77–87 CrossRef Medline
9. Mukherjee, J., Baranwal, A., and Schade, K. N. (2016) Classification of therapeutic and experimental drugs for brown adipose tissue activation: potential treatment strategies for diabetes and obesity. *Curr. Diabetes Rev.* **12,** 414–428 CrossRef Medline
10. Nedergaard, J., Bengtsson, T., and Cannon, B. (2007) Unexpected evidence for active brown adipose tissue in adult humans. *Am. J. Physiol. Endocrinol. Metab.* **293,** E444–52 CrossRef Medline
11. Cypess, A. M., Lehman, S., Williams, G., Tal, I., Rodman, D., Goldfine, A. B., Kuo, F. C., Palmer, E. L., Tseng, Y.-H., Doria, A., Kolodny, G. M., and Kahn, C. R. (2009) Identification and importance of brown adipose tissue in adult humans. *N. Engl. J. Med.* **360,** 1509–1517 CrossRef
12. van Marken Lichtenbelt, W. D., Vanhommerig, J. W., Smulders, N. M., Drossaerts, J. M. A. F. L., Kemerink, G. J., Bouvy, N. D., Schrauwen, P., and Teule, G. J. J. (2009) Cold-activated brown adipose tissue in healthy men. *N. Engl. J. Med.* **360,** 1500–1508 CrossRef
13. Virtanen, K. A., Lidell, M. E., Orava, J., Heglind, M., Westergren, R., Niemi, T., Taittonen, M., Laine, J., Savisto, N.-J., Enerbäck, S., and Nuutila, P. (2009) Functional brown adipose tissue in healthy adults. *N. Engl. J. Med.* **360,** 1518–1525 CrossRef Medline
14. Sidossis, L. S., Porter, C., Saraf, M. K., Børsheim, E., RadhaK. R.ishnan, R. S., Chao, T., Ali, A., Chondronikola, M., Mlcak, R., Finnerty, C. C., Hawkins, H. K., Toliver-Kinsky, T., and Herndon, D. N. (2015) Browning of

subcutaneous white adipose tissue in humans after severe adrenergic stress. *Cell Metab.* **22,** 219–227 CrossRef Medline
15. Kajimura, S., Spiegelman, B. M., and Seale, P. (2015) Brown and beige fat: physiological roles beyond heat generation. *Cell Metab.* **22,** 546–559 CrossRef Medline
16. Wu, J., Boström, P., Sparks, L. M., Ye, L., Choi, J. H., Giang, A.-H., Khandekar, M., Virtanen, K. A., Nuutila, P., Schaart, G., Huang, K., Tu, H., van Marken Lichtenbelt, W. D., Hoeks, J., Enerbäck, S., *et al.* (2012) Beige adipocytes are a distinct type of thermogenic fat cell in mouse and human. *Cell* **150,** 366–376 CrossRef Medline
17. Sharp, L. Z., Shinoda, K., Ohno, H., Scheel, D. W., Tomoda, E., Ruiz, L., Hu, H., Wang, L., Pavlova, Z., Gilsanz, V., and Kajimura, S. (2012) Human BAT possesses molecular signatures that resemble beige/brite cells. *PLoS ONE* **7,** e49452 CrossRef Medline
18. Cannon, B., and Nedergaard, J. (2004) Brown adipose tissue: function and physiological significance. *Physiol. Rev.* **84,** 277–359 CrossRef Medline
19. Ricquier, D. (2011) Uncoupling protein 1 of brown adipocytes, the only uncoupler: a historical perspective. *Front. Endocrinol. (Lausanne)* **2,** 85 CrossRef Medline
20. Shi, F., and Collins, S. (2017) Second messenger signaling mechanisms of the brown adipocyte thermogenic program: an integrative perspective. *Horm. Mol. Biol. Clin. Investig.* **31,** CrossRef CrossRef
21. Collins, S., Yehuda-Shnaidman, E., and Wang, H. (2010) Positive and negative control of Ucp1 gene transcription and the role of β-adrenergic signaling networks. *Int. J. Obes.* **34,** S28–S33 CrossRef
22. Villarroya, F., Peyrou, M., and Giralt, M. (2017) Transcriptional regulation of the uncoupling protein-1 gene. *Biochimie* **134,** 86–92 CrossRef Medline
23. Torres-Quesada, O., Mayrhofer, J. E., and Stefan, E. (2017) The many faces of compartmentalized PKA signalosomes. *Cell Signal.* **37,** 1–11 CrossRef Medline
24. Wong, W., and Scott, J. D. (2004) AKAP signalling complexes: focal points in space and time. *Nat. Rev. Mol. Cell Biol.* **5,** 959–970 CrossRef Medline
25. Rogne, M., and Taskén, K. (2014) Compartmentalization of cAMP signaling in adipogenesis, lipogenesis, and lipolysis. *Horm. Metab. Res.* **46,** 833–840 CrossRef Medline
26. Calejo, A. I., and Taskén, K. (2015) Targeting protein-protein interactions in complexes organized by A kinase anchoring proteins. *Front. Pharmacol.* **6,** 192 CrossRef Medline
27. Tröger, J., Moutty, M. C., Skroblin, P., and Klussmann, E. (2012) A-kinase anchoring proteins as potential drug targets. *Br. J. Pharmacol.* **166,** 420–433 CrossRef Medline
28. Thyagarajan, B., and Foster, M. T. (2017) Beiging of white adipose tissue as a therapeutic strategy for weight loss in humans. *Horm. Mol. Biol. Clin. Investig.* **31,** CrossRef
29. Bonet, M. L., Oliver, P., and Palou, A. (2013) Pharmacological and nutritional agents promoting browning of white adipose tissue. *Biochim. Biophys. Acta* **1831,** 969–985 CrossRef
30. Qiu, Y., Sun, Y., Xu, D., Yang, Y., Liu, X., Wei, Y., Chen, Y., Feng, Z., Li, S., Reyad-Ul Ferdous, M., Zhao, Y., Xu, H., Lao, Y., and Ding, Q. (2018) Screening of FDA-approved drugs identifies sutent as a modulator of UCP1 expression in brown adipose tissue. *EBioMedicine* **37,** 344–355 CrossRef Medline
31. Arch, J. R. S. (2002) β_3-Adrenoceptor agonists: potential, pitfalls and progress. *Eur. J. Pharmacol.* **440,** 99–107 CrossRef Medline
32. de Jong, J. M. A., Larsson, O., Cannon, B., and Nedergaard, J. (2015) A stringent validation of mouse adipose tissue identity markers. *Am. J. Physiol. Endocrinol. Metab.* **308,** E1085–105 CrossRef Medline
33. Roh, H. C., Tsai, L. T. Y., Shao, M., Tenen, D., Shen, Y., Kumari, M., Lyubetskaya, A., Jacobs, C., Dawes, B., Gupta, R. K., and Rosen, E. D. (2018) Warming induces significant reprogramming of beige, but not brown, adipocyte cellular identity. *Cell Metab.* **27,** 1121–1137.e5 CrossRef Medline
34. Huang, D. W., Sherman, B. T., and Lempicki, R. A. (2009) Systematic and integrative analysis of large gene lists using DAVID bioinformatics resources. *Nat. Protoc.* **4,** 44–57 CrossRef Medline
35. Ayroldi, E., Petrillo, M. G., Marchetti, M. C., Cannarile, L., Ronchetti, S., Ricci, E., Cari, L., Avenia, N., Moretti, S., Puxeddu, E., and Riccardi, C. (2018) Long glucocorticoid-induced leucine zipper regulates human thyroid cancer cell proliferation. *Cell Death Dis.* **9,** 305 CrossRef Medline
36. Arasi, F. P., Shahrestanaki, M. K., and Aghaei, M. (2019) A2a adenosine receptor agonist improves endoplasmic reticulum stress in MIN6 cell line through protein kinase A/protein kinase B/Cyclic adenosine monophosphate response element-binding protein/and growth arrest and DNA-damage-inducible 34/eukaryotic initiation factor 2α pathways. *J. Cell. Physiol.* **234,** 10500–10511 CrossRef Medline
37. Cao, W., Daniel, K. W., Robidoux, J., Puigserver, P., Medvedev, A. V., Bai, X., Floering, L. M., Spiegelman, B. M., and Collins, S. (2004) p38 mitogen-activated protein kinase is the central regulator of cyclic AMP-dependent transcription of the brown fat uncoupling protein 1 gene. *Mol. Cell Biol.* **24,** 3057–3067 CrossRef Medline
38. Robidoux, J., Cao, W., Quan, H., Daniel, K. W., Moukdar, F., Bai, X., Floering, L. M., and Collins, S. (2005) Selective activation of mitogen-activated protein (MAP) kinase kinase 3 and p38 MAP kinase is essential for cyclic AMP-dependent UCP1 expression in adipocytes. *Mol. Cell Biol.* **25,** 5466–5479 CrossRef Medline
39. Martinez Molina, D., Jafari, R., Ignatushchenko, M., Seki, T., Larsson, E. A., Dan, C., Sreekumar, L., Cao, Y., and Nordlund, P. (2013) Monitoring drug target engagement in cells and tissues using the cellular thermal shift assay. *Science* **341,** 84–87 CrossRef Medline
40. Lomenick, B., Jung, G., Wohlschlegel, J. A., and Huang, J. (2011) Target identification using drug affinity responsive target stability (DARTS). in *Current Protocols in Chemical Biology*, Vol. **3,** pp. 163–180, John Wiley & Sons, Inc., Hoboken, NJ
41. Merrill, R. A., and Strack, S. (2014) Mitochondria: a kinase anchoring protein 1, a signaling platform for mitochondrial form and function. *Int. J. Biochem. Cell Biol.* **48,** 92–96 CrossRef Medline
42. Carlucci, A., Lignitto, L., and Feliciello, A. (2008) Control of mitochondria dynamics and oxidative metabolism by cAMP, AKAPs and the proteasome. *Trends Cell Biol.* **18,** 604–613 CrossRef Medline
43. Valsecchi, F., Ramos-Espiritu, L. S., Buck, J., Levin, L. R., and Manfredi, G. (2013) cAMP and mitochondria. *Physiology* **28,** 199–209 CrossRef Medline
44. Papa, S., Scacco, S., De Rasmo, D., Signorile, A., Papa, F., Panelli, D., Nicastro, A., Scaringi, R., Santeramo, A., Roca, E., Trentadue, R., and Larizza, M. (2010) cAMP-dependent protein kinase regulates post-translational processing and expression of complex I subunits in mammalian cells. *Biochim. Biophys. Acta* **1797,** 649–658 CrossRef
45. Acin-Perez, R., Gatti, D. L., Bai, Y., and Manfredi, G. (2011) Protein phosphorylation and prevention of cytochrome oxidase inhibition by ATP: coupled mechanisms of energy metabolism regulation. *Cell Metab.* **13,** 712–719 CrossRef Medline
46. Chaudhry, A., Zhang, C., and Granneman, J. G. (2002) Characterization of RII(β) and D-AKAP1 in differentiated adipocytes. *Am. J. Physiol. Cell Physiol.* **282,** C205–12 CrossRef Medline
47. Clapham, J. C. (2004) Treating obesity: pharmacology of energy expenditure. *Curr. Drug Targets* **5,** 309–323 CrossRef Medline
48. Gaundar, S. S., and Bendall, L. J. (2010) The potential and limitations of p38MAPK as a drug target for the treatment of hematological malignancies. *Curr. Drug Targets* **11,** 823–833 CrossRef Medline
49. Wright, M. B., Bortolini, M., Tadayyon, M., and Bopst, M. (2014) Minireview: challenges and opportunities in development of PPAR agonists. *Mol. Endocrinol.* **28,** 1756–1768 CrossRef Medline
50. Psaty, B. M., and Furberg, C. D. (2007) Rosiglitazone and cardiovascular risk. *N. Engl. J. Med.* **356,** 2522–2524 CrossRef Medline
51. Bridges, D., MacDonald, J. A., Wadzinski, B., and Moorhead, G. B. G. (2006) Identification and characterization of D-AKAP1 as a major adipocyte PKA and PP1 binding protein. *Biochem. Biophys. Res. Commun.* **346,** 351–357 CrossRef Medline
52. Vergnes, L., Chin, R., Young, S. G., and Reue, K. (2011) Heart-type fatty acid-binding protein is essential for efficient brown adipose tissue fatty acid oxidation and cold tolerance. *J. Biol. Chem.* **286,** 380–390 CrossRef Medline
53. Uldry, M., Yang, W., St-Pierre, J., Lin, J., Seale, P., and Spiegelman, B. M. (2006) Complementary action of the PGC-1 coactivators in mitochondrial biogenesis and brown fat differentiation. *Cell Metab.* **3,** 333–341 CrossRef Medline
54. Xue, R., Lynes, M. D., Dreyfuss, J. M., Shamsi, F., Schulz, T. J., Zhang, H., Huang, T. L., Townsend, K. L., Li, Y., Takahashi, H., Weiner, L. S., White,

A. P., Lynes, M. S., Rubin, L. L., Goodyear, L. J., *et al.* (2015) Clonal analyses and gene profiling identify genetic biomarkers of the thermogenic potential of human brown and white preadipocytes. *Nat. Med.* **21,** 760–768 CrossRef Medline

55. Plaisier, C. L., Bennett, B. J., He, A., Guan, B., Lusis, A. J., Reue, K., and Vergnes, L. (2012) Zbtb16 has a role in brown adipocyte bioenergetics. *Nutr. Diabetes* **2,** e46 CrossRef
56. Vergnes, L., Davies, G. R., Lin, J. Y., Yeh, M. W., Livhits, M. J., Harari, A., Symonds, M. E., Sacks, H. S., and Reue, K. (2016) Adipocyte browning and higher mitochondrial function in periadrenal but not SC fat in pheochromocytoma. *J. Clin. Endocrinol. Metab.* **101,** 4440–4448 CrossRef Medline
57. Rogers, G. W., Brand, M. D., Petrosyan, S., Ashok, D., Elorza, A. A., Ferrick, D. A., and Murphy, A. N. (2011) High throughput microplate respiratory measurements using minimal quantities of isolated mitochondria. *PLoS ONE* **6,** e21746 CrossRef Medline
58. Schneider, C. A., Rasband, W. S., and Eliceiri, K. W. (2012) NIH Image to ImageJ: 25 years of image analysis. *Nat. Methods* **9,** 671–675 CrossRef Medline
59. Jafari, R., Almqvist, H., Axelsson, H., Ignatushchenko, M., Lundbäck, T., Nordlund, P., and Martinez Molina, D. (2014) The cellular thermal shift assay for evaluating drug target interactions in cells. *Nat. Protoc.* **9,** 2100–2122 CrossRef Medline
60. Rajbhandari, P., Thomas, B. J., Feng, A. C., Hong, C., Wang, J., Vergnes, L., Sallam, T., Wang, B., Sandhu, J., Seldin, M. M., Lusis, A. J., Fong, L. G., Katz, M., Lee, R., Young, S. G., *et al.* (2018) IL-10 signaling remodels adipose chromatin architecture to limit thermogenesis and energy expenditure. *Cell* **172,** 218–233 CrossRef Medline